

2014

Application-Oriented Design and Theoretical Investigation of a Screw-Type Steam Expander

Manuel Grieb

TU Dortmund University, Germany, manuel.grieb@tu-dortmund.de

Andreas Bruemmer

TU Dortmund University, Germany, andreas.bruemmer@tu-dortmund.de

Follow this and additional works at: <https://docs.lib.purdue.edu/icec>

Grieb, Manuel and Bruemmer, Andreas, "Application-Oriented Design and Theoretical Investigation of a Screw-Type Steam Expander" (2014). *International Compressor Engineering Conference*. Paper 2344.
<https://docs.lib.purdue.edu/icec/2344>

This document has been made available through Purdue e-Pubs, a service of the Purdue University Libraries. Please contact epubs@purdue.edu for additional information.

Complete proceedings may be acquired in print and on CD-ROM directly from the Ray W. Herrick Laboratories at <https://engineering.purdue.edu/Herrick/Events/orderlit.html>

Application-Oriented Design and Theoretical Investigation of a Screw-Type Steam Expander

Manuel GRIEB^{1*}, Andreas BRÜMMER²

¹TU Dortmund University, Chair of Fluidics,
Dortmund, Germany
Phone: +49 231 755 5727, Fax: +49 231 755 5722
E-mail: manuel.grieb@tu-dortmund.de

²TU Dortmund University, Chair of Fluidics,
Dortmund, Germany
Phone: +49 231 755 5720, Fax: +49 231 755 5722
E-mail: andreas.bruegger@tu-dortmund.de

* Corresponding Author

ABSTRACT

This paper contains results of an exemplary design and dimensioning process of a screw expander for an organic Rankine cycle for the exhaust heat recovery of internal combustion engines. Both geometric parameters and system parameters are varied in a wide range to maximize overall power output. It is shown that, for small scale applications in particular, a combination of an uncommonly large inner volume ratio with high inlet pressures can be advantageous, despite the fact that only relatively small isentropic expander efficiency is achieved. The remainder of the study includes a consideration of several part load Rankine cycle operation points and presents a method for averaging the final expander size. During the dimensioning process, multi chamber model simulation is used to predict the operation behavior of the screw expander. The multi chamber model of the machine is scaled taking geometrical similarity into consideration (excluding clearance heights) during the simulation process at constant circumferential speed. In this way it is ensured that the actual expander mass flow always matches the calculated ORC mass flow. Moreover, to estimate the overall performance of the heat recovery system and to find common pressure- and speed-dependent operating points for part and full load, a characteristic map of the selected screw expander is calculated.

1. INTRODUCTION

Growing prices of primary energy carriers and increasing environmental requirements lead to the general need to enhance the efficiency of technical systems and exploit the potential of lower energy conversion. A promising approach for both mobile and stationary applications containing internal combustion engines is exhaust heat recovery. Even modern diesel engines only reach efficiency values of approx. 40 % (Schreiner, 2011). Thus a substantial amount of the invested chemical energy is released to the environment as heat losses in the cooling and exhaust system. Overall efficiency can be enhanced by transferring part of this waste heat flow to a coupled organic Rankine cycle in order to vaporize a pressurized working fluid, which drives a heat engine. Screw expanders are highly suitable for the described purpose since they show an auspicious energy conversion in the lower and medium power range with a wide scope of operation (Hütker and Brümmer, 2013).

The crucial factor for achieving sufficient thermal efficiency of the Rankine cycle is expander performance, which can be influenced by choosing the right screw expander geometry as well as by operating the ORC system at an advantageous operation point. An overall system approach for expander design and optimization, which leads to maximal system efficiency but is rather time-consuming, should therefore be favored over an expander-based

approach. This paper presents an approach for an application-oriented design of an exemplary screw-type steam expander for the exhaust heat recovery of heavy truck engines. Influences of ORC parameters and expander geometry on the thermal efficiency of a closed-loop ethanol cycle are discussed and examined by means of multi chamber model simulation.

2. FUNDAMENTALS

2.1 ORC System

The organic Rankine cycle basically has the same working principle as the Clausius Rankine cycle, which converts heat into mechanical work, but an organic fluid with a distinctly lower boiling point is used instead of water. This makes it possible to use heat sources at a relatively low temperature level and therefore offers benefits for waste heat recovery. The liquid working fluid is pumped to an evaporator where a heat flow from the hot exhaust gases is exchanged. After reaching the pressure-dependent boiling temperature, the fluid state changes from liquid to vaporous. Eventually, a superheating is realized. The vapor subsequently flows through an expansion device (a screw-type expander in this particular application) where useful shaft work is converted. Afterwards, the steam is piped through a condenser before it finally reenters the feed pump.

Hot exhaust gases serve as the main heat source for the organic Rankine cycle for the heat recovery of heavy truck engines. Thus the added heat flow depends on exhaust gas conditions and hence on internal combustion engine operation. The definition of thermal efficiency η_{th} for the Rankine cycle is given in equation (1), where \dot{Q}_{exh} is the exhaust gas heat flow, and P_{ORC} is the recovered power, which is composed of effective expander power $P_{e,se}$ and power consumption of the feed pump $P_{e,p}$.

$$\eta_{th} = \frac{P_{ORC}}{\dot{Q}_{exh}} = \frac{P_{e,se} - P_{e,p}}{\dot{Q}_{exh}} \quad (1)$$

The actually exchanged heat flow is affected by pinch point temperature, which is the minimal temperature difference between working fluid and exhaust gas and is typically present at the pressure-dependent boiling point of the working fluid. Assuming there are no heat losses within the system, a certain ORC mass flow \dot{m} can be reached with a defined input heat flow \dot{Q}_{in} , described in equation (2), where h is the specific enthalpy of the working fluid.

$$\dot{m} = \frac{\dot{Q}_{in}}{h_{in,se} - h_{out,p}} \quad (2)$$

In a closed-loop cycle expander outlet pressure $p_{out,se}$ is defined by vapor pressure at condensation temperature, which in turn is affected by the temperature level of the available heat sink. As regards system complexity, it is advantageous to use the cooling system of the combustion engine for that purpose. Assuming that the cooling water temperature is mostly constant, expander outlet pressure can also be regarded as a constant for the whole operation range. The available isentropic power can be determined through knowing the ORC mass flow and the isentropic enthalpy difference as shown in equation (3), where $h_{out,s,se}$ is the specific enthalpy after an isentropic expansion to expander outlet pressure. $h_{in,se}$ is determined with the expander inlet pressure and inlet temperature.

$$P_s = \dot{m}(h_{in,se} - h_{out,s,se}) \quad (3)$$

The presented investigation is carried out with ethanol as the ORC working fluid since it has advantageous properties for this specific case of application, as shown in earlier investigations by Span *et al.* (2011). The maximum steam temperature is set to 550 K to obtain a decomposition temperature safety margin for the working fluid. Moreover, the maximum permitted steam pressure is set to 5 MPa in relation to the mechanical load of the ORC components. Expansion takes place within a single screw expander so as to reduce system complexity.

2.2 Screw Expanders

Screw expanders are two-shaft rotary positive displacement machines with a defined expansion ratio. The characteristic rotor pair is made up of two matching helical screws and is constantly meshed during operation. As the profiled rotor parts are enclosed in a tight housing, working chambers connected in pairs, form between the screw lobes and periodically change their volume as the rotor rotates. Chamber filling and working fluid discharge is controlled by the position of inlet and outlet openings within the casing.

Figure 1 qualitatively shows chamber volume progression as well as the inlet and outlet openings for a working cycle of a screw-type expander. A new chamber emerges between the lobes on the high pressure side of the

expander while the rotors turn in opposite directions. It is connected with the expander inlet port so that working fluid flows in while chamber volume simultaneously increases. The position of the high pressure control edge defines the rotor angular position and the corresponding chamber volume $V_{ex,th}$ at which the filling process stops and the subsequent expansion phase begins. Chamber volume continuously increases during expansion while the chamber in question is ideally isolated from its environment. Thus chamber pressure drops. The leading lobes cross the low pressure control edge of the casing when maximum chamber volume V_{max} is reached and the discharge phase begins in which contained fluid is displaced to the expander outlet while chamber volume simultaneously decreases. The working cycle ends when the chamber in question disappears since screw machines operate without dead spaces. Given that the angular position at maximum chamber volume is affected by screw rotor geometry, the angular position of expansion initiation depends on the inner volume ratio v_i , which is defined in equation (4).

$$v_i = \frac{V_{max}}{V_{ex,th}} \quad (4)$$

The inner volume ratio is a crucial expander parameter because it defines the inner expansion ratio of the screw expander. A large inner volume ratio leads to a shorter filling period and thus to a smaller cross section of the inlet opening. As a result, throttling effects increase during chamber filling. Another effect that impacts working behavior is inevitable leakage through clearances required to separate moving parts from the casing. This can be reduced however by injecting an auxiliary liquid into the working chamber in order to seal clearances.

Like all positive displacement machines, screw expanders change the energy content of a working fluid by performing pressure-volume work, which is finally converted to shaft work. Effective isentropic efficiency $\eta_{e,s}$ is hence defined as shown in equation (5), where M is the torque obtained from the shaft, and ω is the angular velocity.

$$\eta_{e,s} = \frac{P_e}{P_s} = \frac{M \omega}{P_s} \quad (5)$$

The delivery rate λ , which is defined in equation (6), is a measurement for expander mass flow. \dot{m}_{th} is the theoretical mass flow, which would occur in the case of lossless chamber filling without internal leakage meaning that fluid density at expansion start would correspond to inlet conditions $\rho_{in,se}$. Inlet throttling reduces the delivery rate since the actual density at expansion start is lower than in the inlet. Internal leakage on the other hand increases the delivery rate because leakage mass flows are directed in main flow direction.

$$\lambda = \frac{\dot{m}}{\dot{m}_{th}} = \frac{\dot{m}}{V_{ex,th} \rho_{in,se} z_m \omega_m / 2 \pi} \quad (6)$$

Further expander parameters describing the screw geometry are listed below:

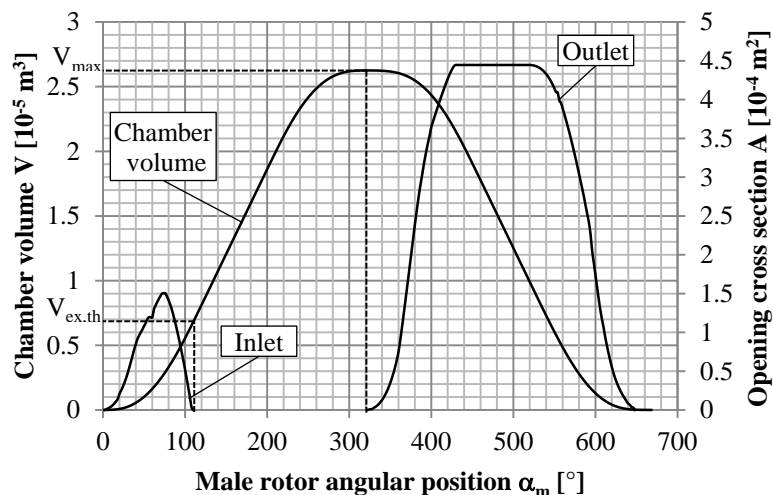


Figure 1: Volume curve and chamber openings for a working cycle of a screw expander

- Rotor profile
- Number of lobes z_m, z_f
- Length diameter ratio of male rotor L_m/D_m
- Wrap angle of male rotor φ_m

Of course, these geometric design parameters and the choice of inner volume ratio affect the operating behavior of screw expanders as they not only specify the size and position of chamber openings and thus the magnitude of inner expansion, but also define the clearance geometry and thus the internal leakage.

2.3 Multi Chamber Simulation

Multi chamber simulation is used to predict the operating behavior of the screw expander, where the screw machine is abstracted to a zero-dimensional time-dependent model, which includes all information. The universal positive displacement machine simulation tool KaSim utilized in this investigation was developed at the Chair of Fluidics of TU Dortmund University. All chambers, chamber connections and miscellaneous capacities are observed simultaneously during thermodynamic simulation. The exchange of mass and energy between chambers or expander ports is considered as well as changes of state through volume alteration. The laws of mass and energy conservation are the basis of the calculation. Simulation results are on the one hand integral values such as expander mass flow or internal power and on the other hand time-dependent pressure and temperature diagrams. (Janicki, 2007), (Kauder *et al.*, 2002)

Designing a screw expander for a closed-loop application requires the expander behavior to be adapted to that of the ORC since the two components are highly depending on another. Steady operation is only possible if the expansion device delivers the evaporated steam flow for the specified system parameters, such as inlet pressure and degree of superheating. Moreover, expander circumferential speed for the design point is determined according to whether a dry running or a liquid-injected screw machine is considered. Thus machine size has to be iteratively adapted during simulation to obtain the intended mass flow with the given circumferential speed. Clearance heights are set to a constant value of $h = 0.1 \text{ mm}$ for this investigation as they only partly depend on machine size. The focus is additionally on liquid-injected machines meaning that the male rotor circumferential speed is set to $c_m = 35 \text{ m/s}$ for the design point. The influence of the injected auxiliary liquid is estimated by sealing 80 % of the housing clearance cross section and 20 % of the cross sections of other clearance types. It is also presumed that, due to throttling effects, only 80 % of the theoretical maximum mass flow will move through inlet and outlet cross sections.

3. APPLICATION-ORIENTED DESIGN APPROACH

A screw machine is traditionally designed focusing on the thermodynamic machine itself. The initial situation is often a defined set of boundary conditions such as mass flow, pressure levels and temperatures, leading automatically to an invariable amount of available isentropic power for energy conversion. In this case, expander design and of expander parameter optimization would equate to maximizing power yield and therefore to maximizing the effective isentropic efficiency factor of the screw-type steam expander. Today, a pressure ratio of up to 15 can be obtained from a single stage oil-flooded industrially manufactured screw compressor (Stosic *et al.*, 2005). Applied by analogy to expanders, this would create an upper bound for expander inlet pressure with a given condensation pressure level. A traditional expander design approach would therefore be to choose one or a few suitable sets of ORC parameters and adapt expander geometry parameters to reach maximal effective isentropic efficiency.

Since optimizing a single part of the ORC system while leaving fluid parameters unchanged does not necessarily mean the whole system's potential is exploited, a system-based approach is suggested where the whole application is considered. Hence the available exhaust gas heat flow is the basis of the expander design process. As favorable ORC parameters such as expander inlet pressure and degree of superheating are still to be determined, the available isentropic power for the expander is not yet specified. The application-oriented design approach basically features a simultaneous variation of expander design parameters and system parameters. The one combination of geometric expander parameters and ORC parameters that provides the highest usable power yield and the highest heat recovery at the same time, has to be identified during the design process. Compared to a traditional design approach, this corresponds to an optimization of thermal efficiency in contrast to an optimization of isentropic expander efficiency.

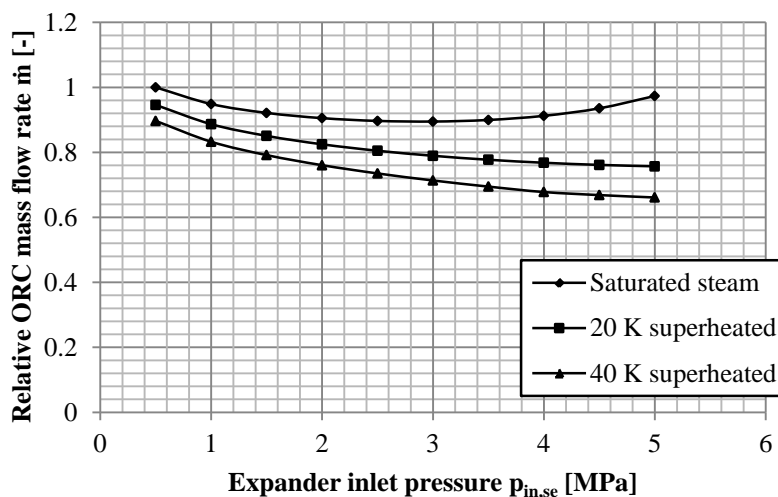


Figure 2: Relative ORC mass flow rate as a function of expander inlet pressure and degree of superheating

3.1 Variation of ORC Parameters

As mentioned before, the ORC parameters are varied at the same time as expander geometry parameters, but in order to provide a general understanding of the system, influences of ORC parameters are presented first of all. In this exemplary design process, expander inlet pressure is altered from 0.5 MPa to 5 MPa for saturated steam and for superheated steam with 20 K and 40 K superheating. For a constant operation of the internal combustion engine, the ORC mass flow can be calculated within this range as shown in Figure 2. Values are related to the maximum mass flow rate. Mass flow rate decreases along with the degree of superheating as a greater specific heat is required to reach the distinct fluid state. For superheated steam, ORC mass flow rate is moderately reduced when expander inlet pressure is increased. However, for a process with saturated ethanol steam, the mass flow rate reaches its minimum at 3 MPa and rises again for greater expander inlet pressures. This is caused by the decreasing slope of the saturation line at higher pressure levels, which becomes lower than those of the lines of constant enthalpy, and evaporation enthalpy drops as a result of this. Consequently, a lower specific heat is necessary to evaporate the working fluid at high pressures. The ORC mass flow rate is a major boundary condition for expander design since it has to match the actual mass flow rate of the screw machine. With the given boundary condition of constant circumferential speed, the mass flow can only be adjusted via geometrical scaling to the designated ORC mass flow rate, which is pressure- and temperature-dependent.

By additionally considering the available isentropic enthalpy difference for a constant expander outlet pressure, the

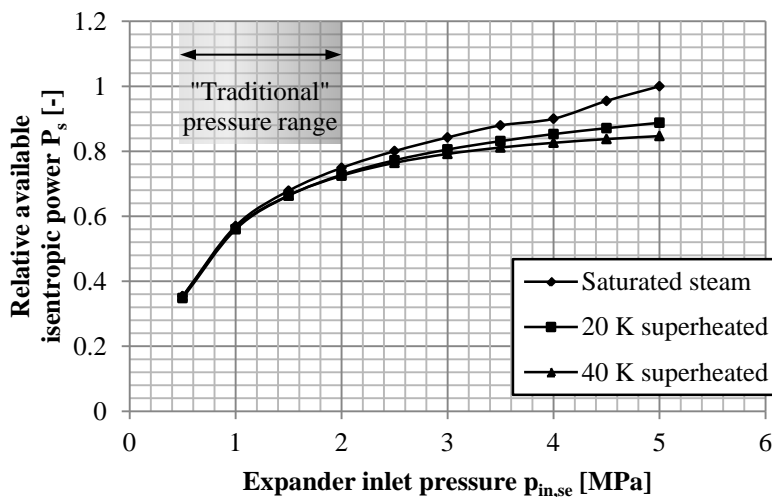


Figure 3: Relative available isentropic power as a function of expander inlet pressure and degree of superheating

available isentropic power for each set of ORC parameters can be determined, as displayed in Figure 3, where data is again related to the maximum value. In general, the available isentropic power of the Rankine cycle increases with expander inlet pressure. The highest value of available isentropic power can be achieved in a saturated steam process. In the higher pressure range, a superheating of the steam reduces isentropic power. As can be seen, the pressure range that offers the best potential for exhaust heat recovery is not accessible with a traditional screw machine design since the pressure ratio is too great. However, this range is purposely included in the remainder of the study.

3.2 Variation of Expander Parameters

Identifying an advantageous expander geometry highly depends on the application, and results differ depending on boundary conditions such as quantity of delivered mass flow rate, working fluid, usage of auxiliary liquids etc. To obtain optimal results, a case specific variation of expander geometry should be implemented. Expander geometry parameters have to be systematically varied along with application parameters. In the preceding sub-section, 30 ORC operation points are dealt with that represent 30 possible design points for the expansion device (for a single operation point of the internal combustion engine). Each screw geometry considered is therefore calculated by means of multi chamber simulation with simultaneous scaling meaning that the delivered mass flow rate corresponds to the previously determined ORC mass flow at a given inlet pressure and temperature. Thus 30 different screw expanders that are geometrically similar (excluding constant clearance heights) are compared where comparability is given by the common amount of waste heat from the truck engine. This procedure ensures that the optimal combination of expander geometry parameters and ORC parameters is detected where utilizable power output is the evaluation criterion.

Figure 4 displays the simulation results for an exemplary expander geometry that has been scaled to all 30 ORC operation points. Hence each data point can be allocated to a distinct dimension of the expander geometry looked at. The size of the expander decreases as the expander inlet pressure or the inlet density increases, and decreases slightly as the degree of superheating progresses, which is mainly due to the decreasing ORC mass flow rate. With this specific expander geometry, the highest usable power is reached with saturated vapor at 5 MPa. A superheating results in a drop of usable power, especially for high expander inlet pressures. Unlike for saturated vapor, a maximum of power forms for superheated steam in the medium pressure range. Usable power is negative for inlet pressures lower than 0.81 MPa, which results through the inner expansion causing a chamber pressure that is lower than the outlet pressure. Expansion shaft work changes its preceding sign when pressure-volume work invested during discharge exceeds that obtained during chamber filling and expansion. For further deliberation, the relative isentropic efficiency for this expander geometry is displayed in Figure 5. In the lower pressure range, results for isentropic efficiency correspond to the trends of usable power. For all degrees of superheating, maxima occur at 2 MPa for the expander geometry in question and isentropic efficiency decreases in the case of a further increase of expander inlet pressure. The best efficiencies ratings can be reached with saturated ethanol steam. The local maximum forms in the pressure range where the inner expansion corresponds to the ORC pressure ratio. An additional reason for the drop in efficiency at higher inlet pressures is that clearance heights are constant while

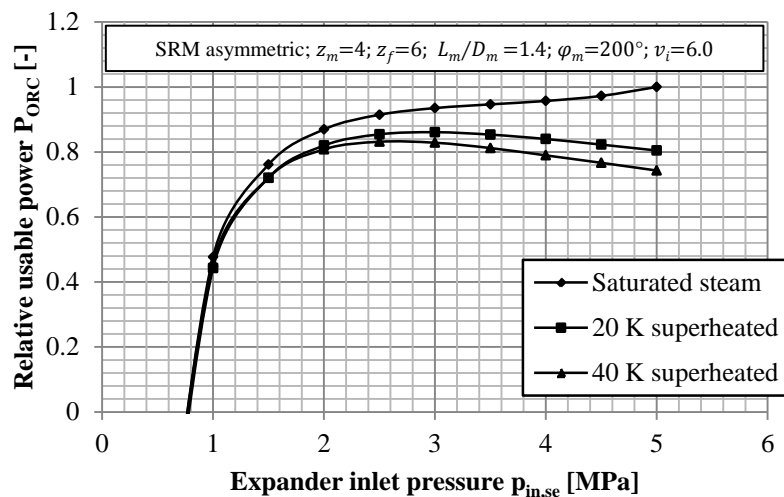


Figure 4: Relative usable ORC power as a function of expander inlet pressure and degree of superheating

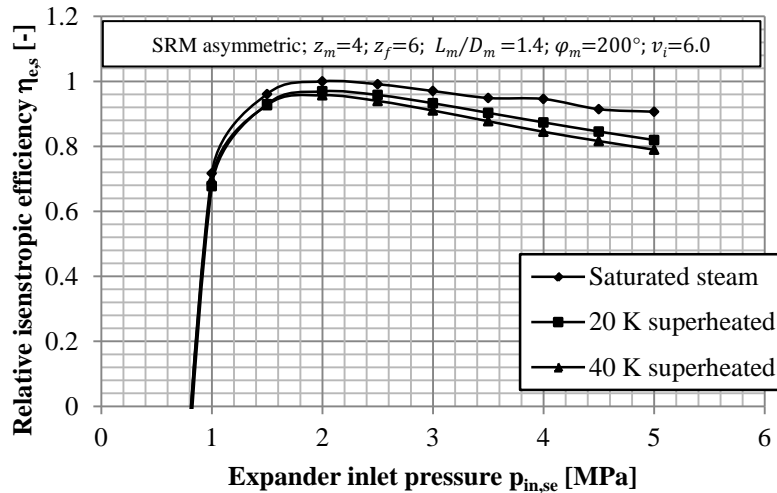


Figure 5: Relative isentropic efficiency as a function of expander inlet pressure and degree of superheating

scaling leads to reduced expander sizes. Consequently, the impact of leakage on energy conversion increases. Although isentropic efficiency ratings of this specific screw expander decrease with high inlet pressures, since the inner expansion ratio is limited and power consumption of the feed pump increases, the highest usable power can be generated with an expander inlet pressure of 5 MPa.

Expander parameters, e.g. inner volume ratio, are varied one after the other in order to find a beneficial design, and the expander geometries are recalculated by means of multi chamber simulation whilst being scaled depending on the ORC mass flow for all 30 ORC operation points. Expander performance is then rated by comparing the maximal usable power output of the different expander geometries within the defined field of ORC parameters. Compared to a traditional design approach, this procedure requires considerably more effort and calculation time, but ensures that expander geometry is optimized in terms of thermal efficiency.

3.3 Evaluation of Expander Performance

It has been shown that expander performance for a single operation point of the combustion engine should be measured in thermal efficiency or in usable power output. Optimizing the isentropic efficiency of the expander does not necessarily lead to an optimization of the overall system performance. Previous content was discussed in the context of a single truck engine operation point. A number of characteristic operation points and related timeframes are identified to represent a realistic driving cycle in order to continue. The general relationships between inlet pressure, inlet temperature and ORC mass flow rate remain, but magnitudes of mass flow rate and available

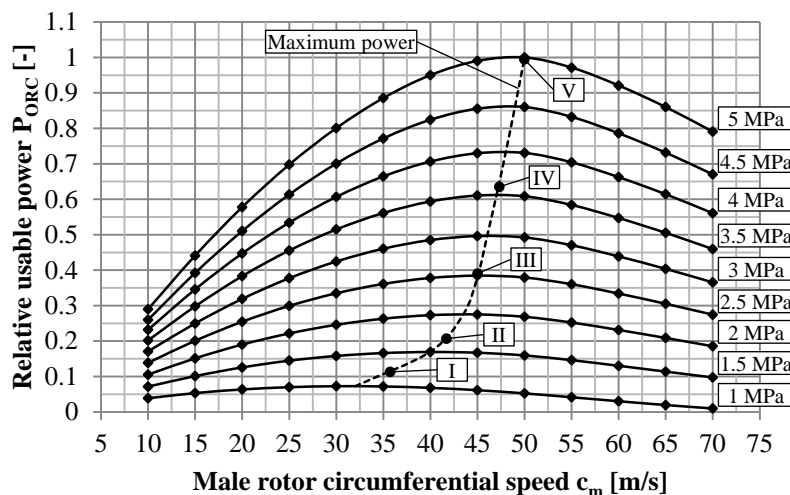


Figure 6: Characteristic map of the screw expander including common operation points (I-V) with truck engine

isentropic power directly depend on the available exhaust gas flow. For the discussed truck application five descriptive part load points are identified and taken into account as soon as during the design process. Again, the thermal efficiency of the ORC should be maximized which corresponds to maximizing the average usable power during the driving cycle. Part load is considered by following the application-oriented design approach presented before for each of the five part load operation points of the ORC. Thus, for each set of expander geometry parameters, a set of five geometrically similar screw machines with different sizes is created (for each of the 30 ORC operation points). The driving cycle time frame and the achieved usable power in the part load point are then used to weight expander volume in order to determine an average expander size.

A characteristic map of the selected screw expander is calculated to find pressure and expander speed-dependent operating points for part and full load and to evaluate the overall performance of the heat recovery system. A final adjustment of expander size is carried out since weighting expander volume represents a compromise. A slight enlargement positively affects the average usable power of the ORC system and enables the system to work at full engine load. A characteristic map of the final expander geometry is presented in Figure 6 where mechanical and fluid friction losses are estimated in accordance with Zellermann's (1996) experimental results. Common operation points exist where delivered expander mass flow and ORC mass flow rate are equal. The inlet pressure and rotational speed of the expander should be selected in such a way that usable power output is maximal for each design point. Inlet pressure and expander speed should thus be controlled along the curve of maximum power, depending on engine operation.

Table 1: Geometry parameters of the final expander design

| | |
|--------------------------|--------------------------------|
| Profile | SRM asymmetric (Schibbye 1979) |
| Number of lobes | $z_m = 4; z_f = 6$ |
| Length to diameter ratio | $L_m/D_m = 1.0$ |
| Male rotor wrap angle | $\varphi_m = 200^\circ$ |
| Inner volume ratio | $v_i = 8.0$ |
| Rotor center distance | 46.2 mm |

4. DESIGN RESULTS

In the scope of this exemplary design process, ten different expander geometries were examined where the inner volume ratio, the length to diameter ratio and the number of lobes were varied systematically. Multi chamber simulation was carried out for all geometries for various ORC parameters, and expander size was iteratively scaled to match the corresponding ORC mass flow rate. In doing so, five operation points of the internal combustion engine were considered and used to average the final expander dimension. In this particular case, expanders with a high inner volume ratio perform promisingly as they allow the high isentropic power available at exceptional high

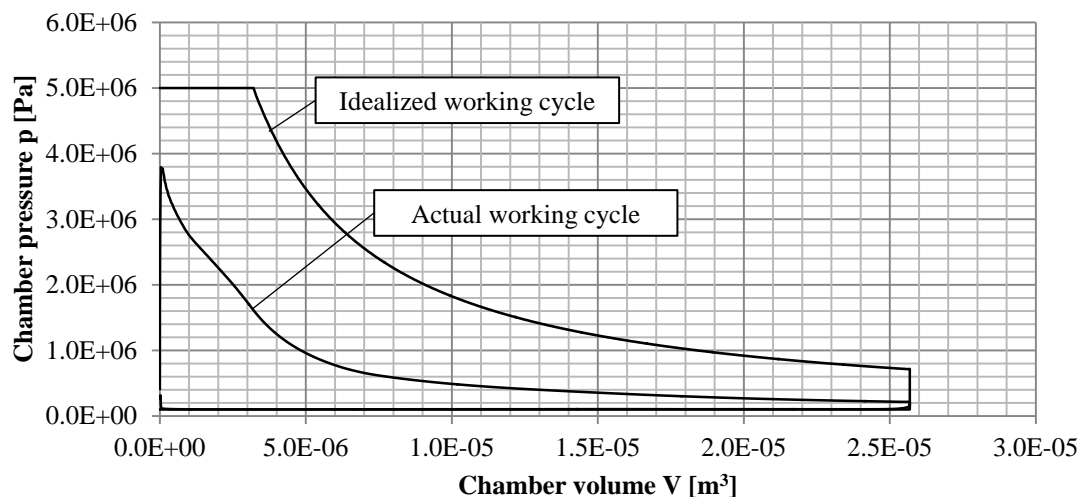


Figure 7: Pressure volume diagram of the final expander design

expander inlet pressures to be used, even though isentropic efficiency only reaches moderate values. The final results of the application-oriented design can be found in Table 1. The high inner volume ratio in particular is a unique feature and marks a significant difference compared to traditionally designed screw machines.

The calculated pressure volume diagram of the final expander design for a circumferential speed of 50 m/s and an inlet pressure of 5 MPa for saturated steam is displayed in Figure 7. An idealized expander working cycle is plotted for the purpose of comparison. At first, the wide discrepancy between calculation results and idealized working cycle is striking. Throttling effects negatively affect the working chamber pressure during the inlet phase. In addition, the immense pressure ratio causes a choked flow through the inlet cross section, and internal leakages reduce the mass that is contained in the chamber. This combined with growing chamber volume affects the given pressure curve. Especially at the time of chamber emergence, when clearances are large compared to chamber volume, pressure decreases substantially. The slope of the pressure curve declines during expansion, and chamber pressure finally drops to low pressure level when the outlet opening is reached at maximum chamber volume. Although leakage flows are directed in main flow direction, a delivery rate of only 40 % is reached at this particular operation point. The influence of inlet throttling clearly outweighs internal leakage. As expander size was scaled to match the ORC mass flow, the low delivery rate was automatically compensated during the application-oriented design process by enhancing expander size. The high usable power output of the expander is hence not only affected by high pressures but to a great extent by the size of the working volume also. The usable power is 17 kW for this operation point.

5. CONCLUSION

In the case of the heat recovery application looked at, the application-oriented design approach targets an optimization of thermal efficiency which corresponds to maximizing usable ORC power output. Throughout the design process, both expander geometry and ORC parameters should be varied systematically so as to examine the full system potential. A traditional design approach most often focuses on optimizing isentropic expander efficiency since the expander is frequently looked at separately from the overall system. This might lead to disadvantageous results for heat recovery applications.

Simulation results show that the available isentropic power increases for saturated ethanol steam at high inlet pressures. Overheating the steam is not advisable as it causes a decrease in ORC mass flow rates. A screw expander with a high inner volume ratio ($v_i = 8$) operating at high inlet pressures of up to 5 MPa promises high thermal efficiency ratings, even though only moderate expander isentropic efficiency ratings can be achieved.

NOMENCLATURE

| | | |
|-----------|-----------------------|----------------------|
| A | Cross section | (m ²) |
| c | Circumferential speed | (m/s) |
| D | Diameter | (m) |
| h | Specific enthalpy | (J/kg) |
| L | Length | (m) |
| \dot{m} | Mass flow | (kg/s) |
| M | Torque | (Nm) |
| ORC | Organic Rankine cycle | (–) |
| p | Pressure | (Pa) |
| P | Power | (W) |
| \dot{Q} | Heat flow | (W) |
| T | Temperature | (K) |
| v_i | Inner volume ratio | (–) |
| V | Volume | (m ³) |
| z | Number of lobes | (–) |
| α | Angular position | (°) |
| η | Efficiency factor | (–) |
| λ | Delivery rate | (–) |
| ρ | Density | (kg/m ³) |
| φ | Wrap angle | (°) |
| ω | Angular velocity | (1/s) |

Subscript

| | |
|-----|----------------------|
| e | Effective |
| ex | Expansion |
| exh | Exhaust gas |
| f | Female |
| in | Inlet |
| m | Male |
| max | Maximum |
| out | Outlet |
| p | Pump |
| s | Isentropic |
| se | Screw expander |
| th | Thermal, theoretical |

REFERENCES

- Hütker, J., Brümmner, A., 2013, Physics of a dry running unsynchronized twin screw expander, *8th International Conference on Compressors and their Systems*, Woodhead Publishing, London, p. 407-416.
- Janicki, M., 2007, *Modellierung und Simulation von Rotationsverdrängermaschinen*, Dissertation, Universität Dortmund, 170 p.
- Kauder, K., Janicki, M., Rohe, A., Kliem, B., Temming, J., 2002, Thermodynamic Simulation of Rotary Displacement Machines, *VDI-Berichte 1715*, VDI Verlag, Düsseldorf, p. 1-16.
- Schibbye, L. B., 1979, Screw-Rotor Machine with Straight Flank Sections, *US Patent 4140445*.
- Schreiner, K., 2011, *Basiswissen Verbrennungsmotor*, Vieweg+Teubner Verlag, Springer Fachmedien Wiesbaden GmbH, Wiesbaden, 236 p.
- Span, R., Eifler, W., Struzyna, R., 2011, Nutzung der Motorabwärme durch Kreisprozesse, *Informationstagung Motoren/Turbomaschinen*, Heft R553, FVV, Bad Neuenahr, 31 p.
- Stosic, N., Smith, I., Kovacevic, A., 2005, *Screw Compressors – Mathematical Modelling and Performance Calculation*, Springer, Berlin, Heidelberg, 138 p.
- Zellermann, R., 1996, *Optimierung von Schraubenmotoren mit Flüssigkeitseinspritzung*, Dissertation, Universität Dortmund, 136 p.

ACKNOWLEDGEMENT

Supported by:

Federal Ministry for Economic Affairs and Energy on the basis of a decision by the German Bundestag